

Lifetime Measurements of Neutron-Rich Light Isotopes ^{14}Be and ^{17}C

M. S. Curtin, L. H. Harwood, J. A. Nolen, B. Sherrill, Z. Q. Xie, and B. A. Brown
National Superconducting Cyclotron Laboratory, Michigan State University, East Lansing, Michigan 48824
 (Received 16 September 1985)

β -decay half-lives have been measured for eight neutron-rich isotopes produced by bombardment of a ^{181}Ta target with an ^{18}O beam at 30 MeV/nucleon. The previously unknown half-lives of ^{14}Be (4.2 ± 0.7 ms) and ^{17}C (202 ± 17 ms) have been obtained along with the half-lives of ^9Li , ^{11}Li , ^{12}Be , ^{12}B , ^{14}B , and ^{15}B . This experiment represents the first half-life measurements using the Michigan State reaction product mass separator.

PACS numbers: 23.40.Hc, 21.60.Cs, 25.70.Np, 27.20.+n

We report here the results of the first half-life measurements of light neutron-rich nuclei using the reaction product mass separator (RPMS) at Michigan State University (MSU). The MSU RPMS is specifically designed for the study of exotic nuclei produced in reactions utilizing intermediate-energy heavy-ion beams.

To permit the study of lifetimes and decay schemes of rare isotopes the RPMS physically separates heavy-ion reaction products of interest from the more abundant isotopes and focuses them to a small spot in the focal plane. The components of the RPMS are indicated schematically in Fig. 1. By eliminating interfering m/q species with defining slits upstream from the focal-plane detector system and concentrating the isotopes under investigation into small detectors, the RPMS provides a relatively background-free environment in which detailed decay studies can be undertaken. A complete description of the RPMS may be found elsewhere.¹

Utilizing a 540-MeV ^{18}O 5+ beam from the K500 cyclotron at the National Superconducting Cyclotron Laboratory, we measured the previously unknown half-lives of ^{14}Be and ^{17}C along with the half-lives of ^9Li , ^{11}Li , ^{12}Be , ^{12}B , ^{14}B , and ^{15}B during a single two-day run. β -decay half-lives were obtained by use of a technique which consisted of repeated measurements of the time interval between the detection of a heavy-ion reaction product and its associated beta particle.

This technique, similar to that employed by Murphy *et al.*,² demonstrated the capability of obtaining half-lives as short as a few milliseconds.

The properties of nuclei far from stability are fundamental to our understanding of nuclear structure in that they provide crucial tests of the validity of shell-model Hamiltonians which have been constructed from data associated with near-stable nuclei. Beta-decay properties of neutron-rich systems are of particular importance because they provide opportunities to nearly isolate specific one-body transition terms which either do not occur with significant intensity in existing near-to-stability nuclei or are masked by mixing with other terms. As the predictive capability of shell-model calculations improve comparisons between predicted and measured properties may yield discrepancies which can only be explained as a breakdown in the model-space assumptions. For instance, Hamiltonians generated within the context of a spherical shell-model basis set can lead to large discrepancies between experiment and theory which may indicate the onset of new regions of deformation as was the case for neutron-rich sodium and magnesium isotopes.³

Neutron-rich isotopes were produced by bombardment of targets of beryllium and tantalum with a 30-MeV/nucleon ^{18}O beam. Target thickness was chosen so as to eliminate the primary beam while allowing the neutron-rich fragments to pass through the target and

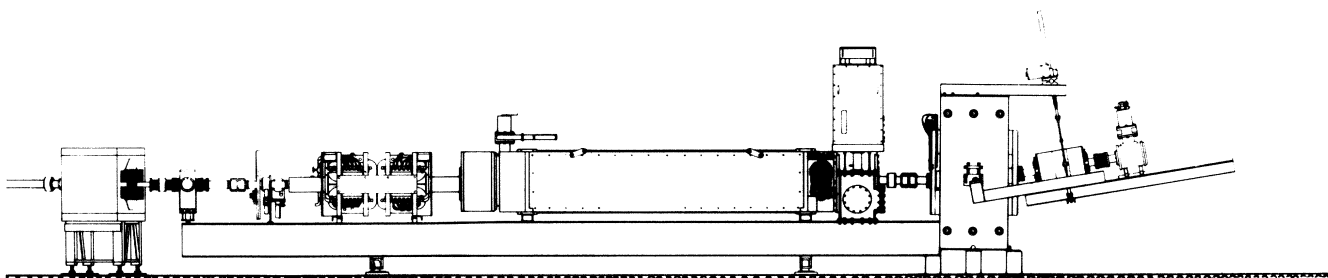


FIG. 1. Pictorial drawing of the RPMS. The beam inflector magnet is the first component at the left, followed by the bellows system and target chamber, aperture holder, quadrupole doublet, Wien filter (5 m long) with high-voltage supplies on the top right-hand end, magnetic dipole, and pivoting "tail" with quadrupole doublet and focal-plane detectors at the right-hand end.

into the RPMS, which was positioned at a scattering angle of 0° . The yield of neutron-rich isotopes was substantially greater for the tantalum targets than for the beryllium targets, which proved consistent with preliminary results reported by Guerreau *et al.* using 44-MeV/nucleon beams.⁴ Reaction products were separated and focused according to their mass-to-charge ratio into a focal-plane detector system consisting of a two-dimensional position-sensitive gas-proportional counter followed by a ΔE - E solid-state detector telescope. Horizontal and vertical position information was obtained in the gas counter through resistive-wire charge division and electron drift times, respectively. The ΔE - E telescope provided isotope identification and consisted of a $300\text{-mm}^2 \times 100\text{-}\mu\text{m}$ (Si) detector backed by a $500\text{-mm}^2 \times 5\text{-mm}$ (Si-Li) detector. During the experiment, lifetime measurements were carried out by turning off the beam whenever an ion with $Z \geq 3$ was detected in the ΔE - E telescope thus allowing the decay time of that ion to be recorded. Elimination of the beam was accomplished within $40 \mu\text{s}$ of the detection of a heavy-ion reaction product by a change of the rf phase on one of the dees in the K500 cyclotron. The duration of the beam-off time interval was chosen to be several half-lives of the longest-lived beta-decaying species hitting the detector system, thereby eliminating the buildup of noninteresting isotopic species within the detector system. A scalar was used to record pulses from an 8192-Hz quartz-crystal oscillator during the time period between the observation of a heavy-ion reaction product (tagged as a beam-on event) and its associated beta particle (tagged as a beam-off event). The data associated with heavy-ion reaction products and their decay products were written to tape for final analysis at a later date.

The off-line analysis consisted of a histogramming of the time-interval distribution between the detection of a heavy-ion reaction product and its corresponding beta particle. Isotope identification was achieved by the coupling of m/q information (contained in the vertical-position signal) with a particle identification (PI) function assumed to obey the empirical relation²

$$F_{PI} = (E + \Delta E)^{1.78} - E^{1.78},$$

which was evaluated with use of the energy information from the ΔE - E telescope. Histogramming of two-dimensional focal-plane position vs F_{PI} produces islands corresponding to different isotopic species as shown in Fig. 2. The adjustable dispersion of the RPMS coupled with a set of horizontal defining slits located just in front of the focal-plane detector system proved an effective combination for the elimination of isotopes with undesirable m/q values.

For the $m/q = 3$ analysis, beta particles were required to lose more than ~ 2.5 MeV in the E detector

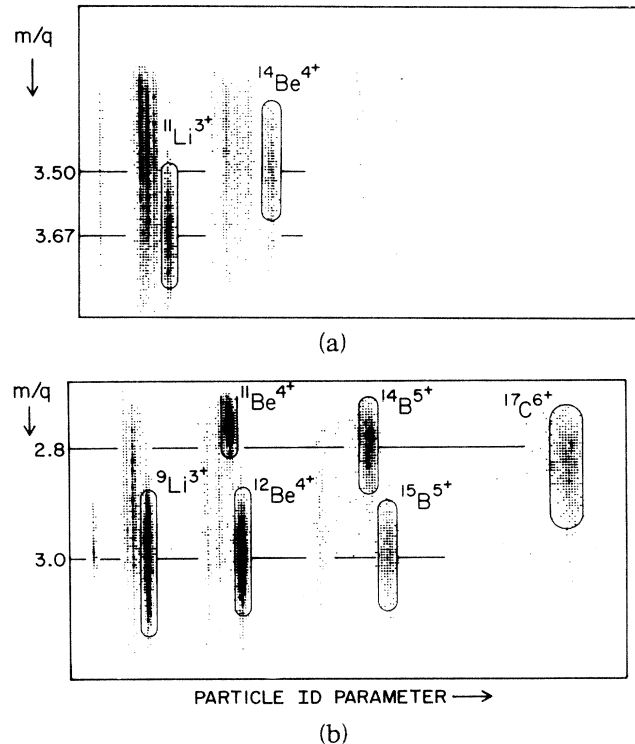


FIG. 2. Two-dimensional histograms providing particle identification for $Z \geq 3$. (a) Particle identification for the $m/q = 3.5$ run. (b) Particle identification for the $m/q = 3.0$ run.

to be included in the lifetime curve so as to eliminate background events associated with ^6He . For the $m/q = 3.5$ run ^6He was eliminated by the brass defining slits, thus allowing the beta energy threshold to be reduced to ~ 1.0 MeV. The remaining background was small and believed to arise from long-lived species embedded in the detector during previous beam-on cycles. The decay curves of ^9Li , ^{11}Li , ^{14}B , ^{15}B , and ^{17}C were fitted as an exponential decay plus constant background with use of a least-squares fitting routine. The decays of ^{14}Be and ^{12}Be were complicated by a relatively short-lived daughter product. For such mother-daughter decays we required a second beta to follow the first beta particle within approximately two daughter half-lives in order for it to be included in the mother's decay curve. The daughter's half-life was also extracted by the histogramming of the time-interval distribution between the first and second beta particles. The resulting histograms are presented in Fig. 3 along with their best-fit curves.

The present experimental results are compared with previous measurements in Table I. There are two cases of discrepancies outside the one-standard-deviation uncertainties, ^{14}B and ^{15}B . In both of these cases there was only one previous measurement, and there is no obvious reason for the discrepancies. It is

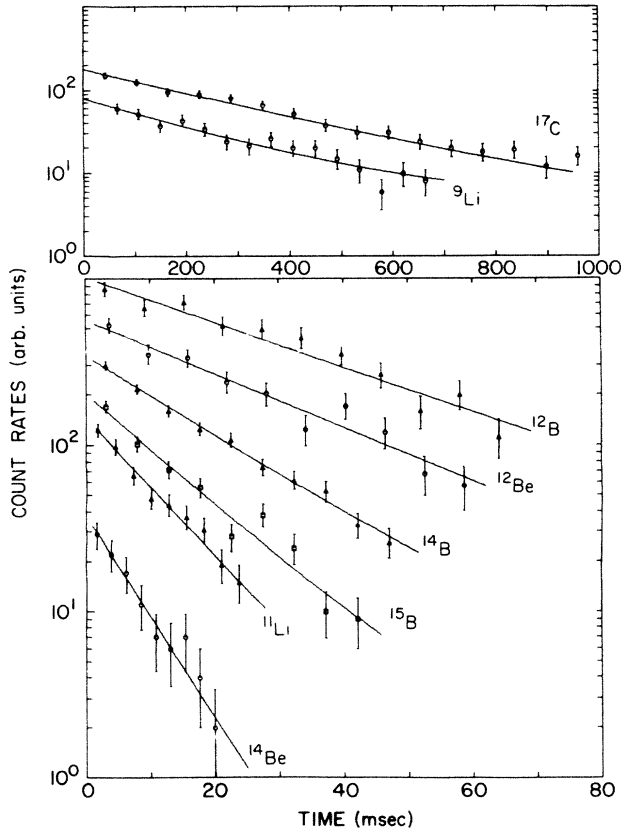


FIG. 3. The beta-decay half-life data from this experiment along with their best-fit curves. The curves represent least-squares fits to the data with assumption of a functional form given by a simple exponential plus a constant background. In each case the time scale for the data extend to larger times than displayed in this figure in order to determine the background accurately.

possible that the background under the ^{14}B decay curve in Ref. 7 was underestimated, leading to the larger value for the extracted lifetime. In Ref. 8 no decay curve for ^{15}B was shown so that it is hard to compare the quality of the fits in this case.

For the neutron-rich nuclei investigated in this experiment the dominant decay mode is through Gamow-Teller beta decay. Partial half-lives corresponding to Gamow-Teller beta decay are predicted within the framework of a spherical shell-model formalism (details of which are given in Ref. 9). Shell-model calculations were carried out in the PSD model space in which the $0p_{3/2}$, $0p_{1/2}$, $0d_{5/2}$, $1s_{1/2}$, and $0d_{3/2}$ orbitals are active. The residual-interaction matrix elements connecting the $0p$ -shell orbits were taken from the results of a fit to $0p$ -shell energy levels in the $A=10-15$ mass region obtained by Millener.¹⁰ The matrix elements connecting the $1s0d$ -shell orbitals were taken from the recent fit to $1s0d$ -shell energy levels in the $A=18-38$ mass region obtained by Wil-

TABLE I. Beta-decay half-lives (in milliseconds) for the neutron-rich isotopes measured in this experiment compared with previous measurements when they exist. Theoretical predictions for Gamow-Teller beta decay are also provided for comparison. The three theoretical half-lives for ^{17}C correspond to the assumption of $(\frac{1}{2}^+, \frac{3}{2}^+, \frac{5}{2}^+)$ ground-state J^π values for ^{17}C in the calculation.

Isotope	This measurement	Previous measurement	Prediction ^a
^9Li	173 ± 14	175 ± 1^b	76
^{11}Li	7.7 ± 0.6	8.5 ± 0.2^b	2.3
^{12}Be	21.3 ± 2.2	24.4 ± 3.0^c	8.6
^{14}Be	4.2 ± 0.7	. . .	2.8
^{12}B	20.0 ± 1.5	20.41 ± 0.06^d	13.6
^{14}B	12.8 ± 0.8	16.1 ± 1.2^e	11.1
^{15}B	8.8 ± 0.6	11.0 ± 1.0^f	7.4
^{17}C	202 ± 17	. . .	(422, 297, 242)

^aPresent calculations.

^bReference 3.

^cReference 5.

^dReference 6.

^eReference 7.

^fReference 8.

denthal.¹¹ Finally, cross-shell matrix elements connecting both the $0p$ and $1s0d$ orbitals were calculated with the residual interaction of Millener and Kurath.¹² Single-particle energies were chosen to reproduce single-particle states in $A=17$ nuclei and single-hole states in $A=15$ nuclei with the assumption of a closed $0s0p$ shell configuration for ^{16}O . Half-lives predicted by these calculations are presented in Table I.

On the basis of the systematics of the comparisons between experimental Gamow-Teller beta decay strengths and those calculated with similar types of shell-model wave functions to those employed here (see Brown and Wildenthal¹³ and Snover *et al.*¹⁴), we expect about a 60% reduction of the decay strength or a corresponding 67% increase in the half-life. In Table I we find that only the half-life of ^{12}B , which lies closest to the value of stability, is in accordance with this expectation. The experimental half-lives for ^9Li , ^{11}Li , and ^{12}Be are all over a factor of 2 larger than theory. Our model space for these nuclei is restricted to the $0p$ shell. Any larger than average $1s0d$ shell admixtures in the initial state could explain the longer than average half-life, since these components cannot contribute to the transition to the final state. Indeed, it is well known that some $0s1d$ configurations occur very low in excitation energy in this mass region and even appear as the ground state in ^{11}Be . A similar effect occurs in the most neutron-rich Na and Mg isotopes (see Fig. 1 of Ref. 9) presumably because of a close degeneracy between $0p1f$ and $1s0d$ configurations. This shortcoming of our calculation can only be improved if we allow for some $0s1d$ admixtures in our

model space.

In contrast, the experimental half-lives of the nuclei with $N > 8$ (^{14}B , ^{15}B , and ^{17}C) are closer to the theory and even smaller than theory in the case of ^{17}C . In our model space, these nuclei all have the active protons in the $0p$ shell and the active neutrons in the $1s0d$ shell. These half-life discrepancies, as well as other problems associated with this type of configuration (Ref. 14), might be improved by a better determination of the cross-shell residual interaction between protons and neutrons. In order to do this it is important to have as much information as possible on the energy levels in this region with $Z < 8 < N$, and a measurement of the final-state decay schemes for the nuclei which can be studied with the RPMS would be invaluable in this regard.

In conclusion, the first half-life measurements of light neutron-rich nuclei using the MSU reaction product mass separator has resulted in the measurement of eight half-lives, two of which represent first-time measurements and three of which are second-time measurements. All beta-decay histograms presented in Fig. 3 were obtained during ten hours of data taking. The RPMS proved extremely effective in the elimination of unwanted reaction products at the focal-plane detector system, thus providing a relatively background-free decay curve. The measurement technique demonstrated the possibility of determining half-lives as short as a few milliseconds. Future studies on the beta decay of exotic nuclei will be aimed at providing branching-ratio information against which shell-model calculations may be more vigorously tested.

This work is supported by the National Science Foundation through Grant No. PHY 83-12245.

¹L. H. Harwood and J. A. Nolen, Jr., Nucl. Instrum. Methods **186**, 435 (1981); J. A. Nolen, Jr., L. H. Harwood, M. S. Curtin, E. Ormand, and S. Bricker, in *Proceedings of the Conference on Instrumentation for Heavy-Ion Nuclear Research, Oak Ridge, Tennessee, 1984*, edited by D. Shapiro (Harwood Academic, New York, 1985).

²M. J. Murphy, T. J. M. Symons, G. D. Westfall, and H. J. Crawford, Phys. Rev. Lett. **49**, 455 (1982).

³E. Roeckl, P. F. Dittner, C. Detraz, R. Klapisch, C. Thibault, and C. Rigaud, Phys. Rev. C **10**, 1181 (1974).

⁴D. Guerreau, V. Borrel, D. Jacquet, J. Galin, B. Gatty, and X. Tarrago, GANIL Report No. IPNO DRE 83-19 (to be published).

⁵D. E. Alburger *et al.*, Phys. Rev. C **17**, 1525 (1978).

⁶F. Ajzenberg-Selove, Nucl. Phys. **A248**, 1 (1975).

⁷D. E. Alburger and D. R. Goosman, Phys. Rev. C **10**, 912 (1974).

⁸J. P. Dufour *et al.*, Centre d'Etudes Nucléaires de Bordeaux-Gradignan Report No. CENBG 8430 (to be published).

⁹B. H. Wildenthal, M. S. Curtin, and B. A. Brown, Phys. Rev. C **28**, 1343 (1983). The beta-decay phase factors were evaluated with use of Q values given by A. H. Wapstra and G. Audi, Nucl. Phys. **A432**, 1 (1985), and excitation energies for the final states from experiment when given in *Table of Isotopes*, edited by C. M. Lederer and V. S. Shirley (Wiley, New York, 1978), or theoretical excitation energies otherwise. The Gamow-Teller matrix elements were calculated with the "free-nucleon" operator.

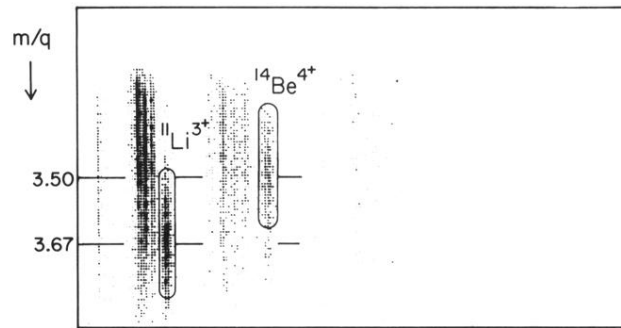
¹⁰D. J. Millener, private communication.

¹¹B. H. Wildenthal, *Progress in Particle and Nuclear Physics* (Pergamon, New York, 1983), Vol. 11, p. 5.

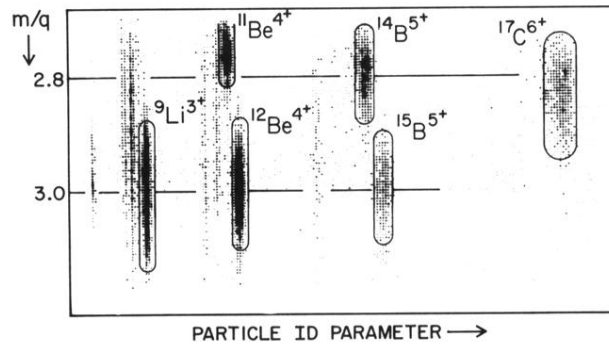
¹²D. J. Millener and D. Kurath, Nucl. Phys. **A255**, 315 (1975).

¹³B. A. Brown and B. H. Wildenthal, Phys. Rev. C **28**, 2397 (1983), and to be published.

¹⁴K. A. Snover, E. G. Adelberger, P. G. Ikossi, and B. A. Brown, Phys. Rev. C **27**, 1837 (1983).



(a)



(b)

FIG. 2. Two-dimensional histograms providing particle identification for $Z \geq 3$. (a) Particle identification for the $m/q = 3.5$ run. (b) Particle identification for the $m/q = 3.0$ run.